Universiteit Antwerpen

This item is the archived peer-reviewed author-version of:

Novel 2-naphthyl substituted zinc naphthalocyanine : synthesis, optical, electrochemical and spectroelectrochemical properties

Reference:

Dubinina T.V., Moiseeva E.O., Astvatsaturov D.A., Borisova N.E., Tarakanov P.A., Trashin Stanislav, De Wael Karolien, Tomilova L.G..- Novel 2-naphthyl substituted zinc naphthalocyanine : synthesis, optical, electrochemical and spectroelectrochemical properties
New journal of chemistry - ISSN 1144-0546 - 44:19(2020), p. 7849-7857
Full text (Publisher's DOI): https://doi.org/10.1039/D0NJ00987C
To cite this reference: https://hdl.handle.net/10067/1689520151162165141

uantwerpen.be
Institutional repository IRUA

Please do not adjust margins

ARTICLE

Novel 2-naphthyl substituted zinc naphthalocyanine: synthesis, optical, electrochemical and spectroelectrochemical properties

Received 00th January 20xx,
Accepted 00th January 20xx

DOI: 10.1039/x0xx00000x

T.V. Dubinina,[a,b]* E.O. Moiseeva,[a] D.A. Astvatsaturov,[a] N.E. Borisova,[a,c] P.A. Tarakanov,[b] S.A. Trashin,[d,e] K. De Wael,[d,e] L.G.Tomilova [a,b]

Novel near IR absorbing zinc 2,3-naphthalocyanine with bulky 2-naphthyl groups was obtained from corresponding 2,3-dicyanonaphthalene and characterized by mass spectrometry, UV-Vis, infrared and nuclear magnetic resonance spectroscopy (NMR). Two-dimensional NMR was employed for full proton and carbon signal assignment in initial 2-naphthyl-substituted 2,3-dicyanonaphthalene. The main absorption maximum of 2-naphthyl-substituted naphthalocyanine complex at 790 nm shows a shift of 6 nm to the near IR region compared to phenyl-substituted analogues. The UV-Vis spectrum of the complex in *o*-DCB shows strong aggregation, which can be suppressed by N-containing agents or ternary ammonium salt due to steric hindrance or electrostatic repulsion. Pyridine demonstrates the most pronounced effect that reaches maximum value at 2vol% pyridine. The monomeric form of the naphthalocyanine complex has a narrow *Q* band and well-resolved satellites. Since pyridine may play a role of both coordinating and reducing agent, fluorescence and electron paramagnetic resonance spectroscopy were used to clarify the mechanism of its influence on the naphthalocyanine complex. Fluorescence properties (fluorescence and excitation spectra, fluorescence quantum yield) as well as electrochemical and spectroelectrochemical behavior were studied in *o*-DCB. The addition of pyridine results in slight shift towards a higher value for the first oxidation and first reduction potentials. Moreover, the first oxidation process shows a split that increases after the addition of pyridine. Nevertheless, a single reversible one-electron transition was confirmed by spectroelectrochemical titration in the region of the first oxidation. The first oxidation process of the naphthalocyanine complex was accompanied by reversible color change from olive to bright green, which is not typical for naphthalocyanine complexes with other functional groups (e.g. unsubstituted, alkyl, alkoxy, aryl).

Introduction

2,3-Naphthalocyanines are analogues of phthalocyanines with an extended aromatic system that leads to about 100 nm red shift of the main absorption band compared to phthalocyanine complexes. Known as the rule of "100 nm" [1, 2], this shift results from the destabilization of the HOMO level and the corresponding decrease in the HOMO-LUMO gap in 2,3-naphthalocyanines [3]. Thus, naphthalocyanines and their metal complexes possess high extinction coefficients in the near IR region, making them promising materials for photodynamic therapy applications (due to deep penetration of near IR light into mammalian tissues) [4-6] and photoactive layers in solar cells (due to covering a near IR part of the solar spectrum) [7, 8].

Destabilization of the HOMO level causes a decrease of the first oxidation potential of naphthalocyanine complexes compared to phthalocyanines [3, 9]. Due to this peculiarity naphthalocyanines demonstrate facile, reversible and contrast color change upon oxidation, which is of importance for the development of electrochromic devices [10-12].

In contrast, naphthalocyanine complexes are considered to be poorly stable in solution in the presence of oxygen because of a comparatively low oxidation potential. Due to the photosensitizing properties of the complexes mediated by singlet oxygen [13], light can also influence their stability. Singlet oxygen may attack electron-reach aromatic bounds with formation of corresponding endoperoxides and further cleavage of C-C bond [13, 14].

However, comparing to their linear benzoannelated analogues called antracocyanines, naphthalocyanines demonstrate higher stability to oxidation by atmospheric oxygen both in solution and in solid state. For instance, naphthalocyanine complexes can be stored unchanged in aerobic conditions in solid state for years. In turn, antracocyanines are very unstable and, should be stored in dark under nitrogen but the most of them usually oxidize despite these efforts [3].

b. Department of chemistry, Lomonosov Moscow State University, 119991 Moscow, Russian Federation.
b. Institiute of physiologically Active Compounds, Russian Academy of Science, 142432 Chernogolovka, Moscow Region, Russian Federation.
c. A.N. Nesmeyanov Institute of Organoelement Compounds Russian Academy of Science, 28 Vavilov Str. 119334 Moscow, Russian Federation
d. AXES research group, Groenenborgerlaan 171, University of Antwerp, 2020 Antwerp, Belgium.
e. Nanolab Center of Excellence, Groenenborgerlaan 171, University of Antwerp, 2020 Antwerp, Belgium.
@Corresponding author E-mail: dubinina.t.vid@gmail.com
Electronic Supplementary Information (ESI) available: [details of any supplementary information available should be included here]. See DOI: 10.1039/x0xx00000x

Please do not adjust margins

Please do not adjust margins

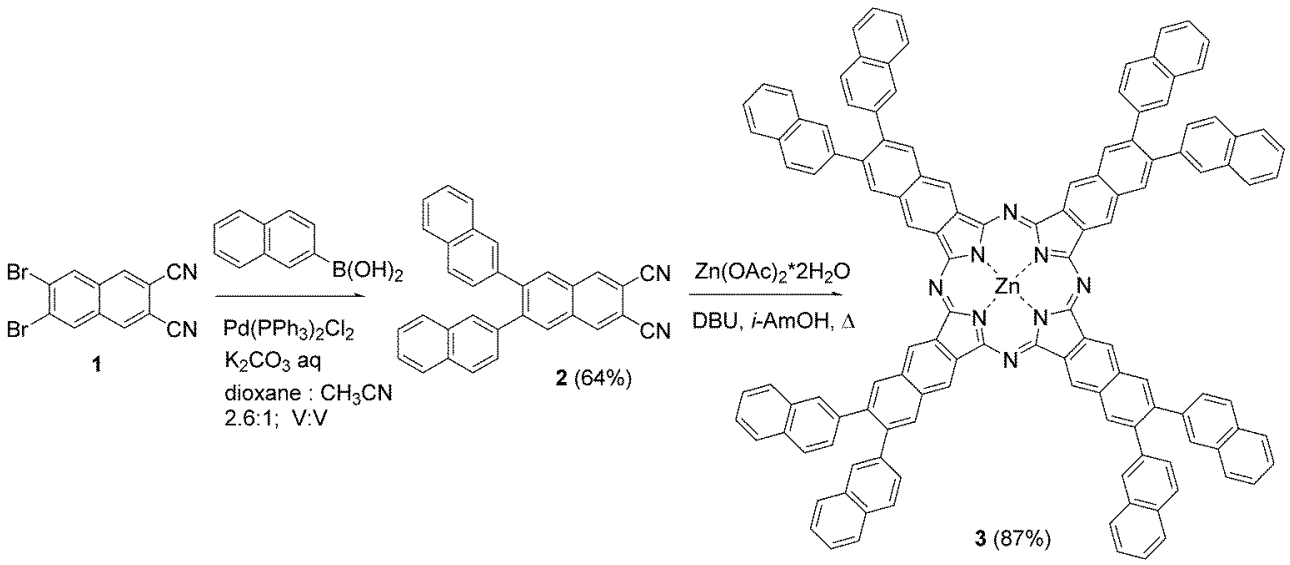

Scheme 1. Synthesis of naphthalocyanine complex **3**.

Thus, among of π-extended phthalocyanine analogues naphthalocyanine complexes are the most stable near IR absorbing materials.

Extension of the π-system promotes intermolecular π-stacking interactions and aggregation of naphthalocyanines in non-coordinating solvents (*e.g., o*-DCB) especially in saturated solutions (c ≥ 10^{-4} M). In some cases, the aggregation/disaggregation processes accompany with change of color [15, 16].

Noteworthy, peripheral functional groups in naphthalocyanine macrocycle also affect the extent of inter- and intramolecular interactions and physicochemical properties of naphthalocyanine complexes. In order to overcome aggregation bulky substituents should be introduced to the naphthalocyanine moiety. Additionally, for disaggregation in saturated solutions, the coordinating additives should be employed (*e.g.,* N or O-ligands, such as alkylamines or THF) [17]. Coordination of these compounds to the central ion in a naphthalocyanine molecule leads to steric hindrance or electrostatic repulsion and disaggregation.

In this work, we introduced bulky aromatic 2-naphthyl groups into naphthalocyanine macrocycle in order to investigate the influence of π-system extension in peripheral groups on spectral and electrochemical properties of corresponding naphthalocyanine complexes. We also investigated the influence of strongly coordinating agents as disaggregation additives to the optical and electrochemical behavior of the naphthalocyanine.

Results and discussion

6,7-Bis(2-naphthyl)naphthalene-2,3-dicarbonitrile was achieved through Suzuki cross-coupling reaction between 6,7-dibrom-2,3-dicyanonaphthalene **1** and 2-naphthyl boronic acid. The mixture of 1,4-dioxane and acetonitrile was chosen as a solvent as the presence of acetonitrile leads to a good solubility of the initial 6,7-dibrom-2,3-dicyanonaphthalene in the reaction mixture. In order to prevent the formation of undesirable mono-naphthyl-substituted product, the following terms should be held. Firstly, boronic acid should be introduced to the reaction mixture in 6 fold excess. A similar ratio of initial compounds was employed to obtain 3-ethylthiophenyl substituted naphthalene-2,3-dicarbonitrile [18] and phenyl substituted phthalonitrile [19]. Secondary, K_2CO_3 should be dissolved in sufficient quantity of water for preparation of saturated solution and the reaction mixture should be stirred vigorously. The main advantage of using a Pd(II) catalyst is its stability during the storage.

In comparison with phenyl-substituted analogues, described by us earlier [9], the employment of sterically hindered boronic acids in the Suzuki cross-coupling reaction decreases the yield of target compounds. In the case of phenyl-substituted phthalonitrile and corresponding naphthalene-2,3-dicarbonitrile, yields lay in the range 75-85%. For bulky 2-naphthyl and 3-(ethylthio)phenyl [18] groups, yields decreased to 64-66%.

The naphthalocyanine complex was obtained from dinitrile **2** in boiling isoamyl alcohol using template approach in the presence of 1,8-diazabicycloundec-7-ene (DBU) as a base. The reaction was conducted under an inert atmosphere to protect naphthalocyanine **3** from oxidation by atmospheric oxygen under the conditions of boiling reaction mixture.

The structures of initial dinitrile **2** and naphthalocyanine complex **3** were confirmed using NMR and IR spectroscopy and mass-spectrometry.

During the assignment of carbon signals in NMR spectra of compound **2,** we faced a problem of overlay of some signals. In order to assign the signals precisely, ^{1}H-^{13}C HSQC and ^{1}H-^{13}C HMBC spectra were registered (Figure S1 and Figure S2). The following signals of C^7, C^8 and C^{10} lie within a narrow region from 127.34 ppm to 127.46 ppm.

This journal is © The Royal Society of Chemistry 20xx

Please do not adjust margins

Please do not adjust margins

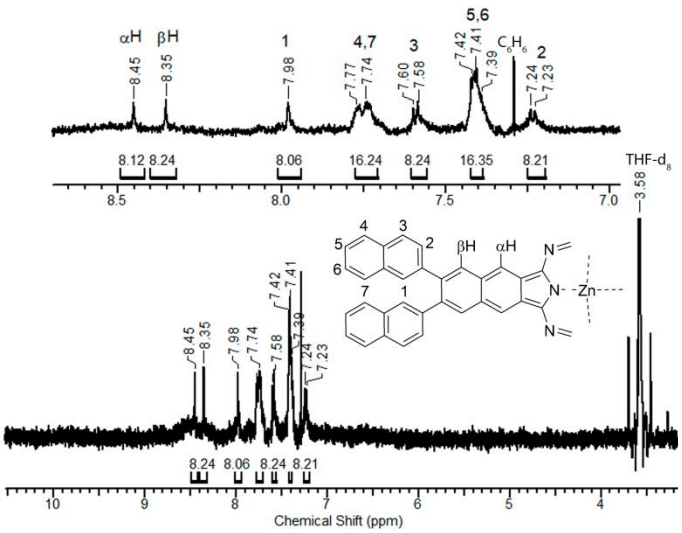

Figure 1. ^{1}H NMR spectrum of naphthalocyanine complex **3** in THF-d_8. Full spectrum (upper image) and enlarged aromatic region (bottom image) are presented.

Table 1. ^{1}H NMR data for compound **3** and some aryl-substituted 2,3-naphthalocyanine complexes.

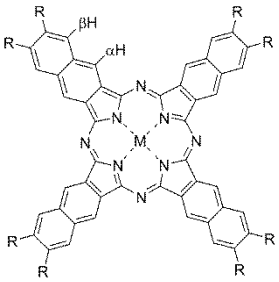

Compound	R	M	δ(H_{Ar}), ppm	δ(βH), ppm	δ(αH), ppm	Solvent
3	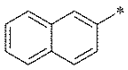	Zn	7.23-7.98	8.35	8.45	THF-d_8
^{Ph8}NcMg [20]	C_6H_5	Mg	7.33-7.39	8.21	8.66	Py-d_5
^{PhO8}NcMg [12]	OC_6H_5	Mg	7.18-7.42	8.03	9.54	THF-d_8
^{EtSPh8}NcZn[18]	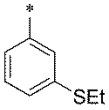	Zn	7.35-7.46	8.47	9.27	THF-d_8
^{Ar8}NcZn [21]	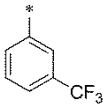	Zn	7.54-7.75	8.50	9.30	THF-d_8

Additionally, a partial overlay of the signals of C^{11} and C^{12} was found at 126.47-126.51 ppm. And there are some complex overlaying multiplets of proton signals H^{10} and H^{13}, H^{11} and H^{12}. For instance, the multiplets of H^{10} and H^{13} and corresponding carbon atoms were demarcated using the presence of correlation between H^{13} and C^{15}; H^{10} and C^{8} in ^{1}H-^{13}C HMBC spectrum (Figure S2). The multiplets of H^{11} and H^{12} and corresponding carbon atoms were demarcated using the presence of correlations between H^{11} and C^{9}; H^{12} and C^{14}.

In the case of naphthalocyanine complex **3**, NMR spectrum was measured in polar, coordinated solvent (THF) with the aim of achieving disaggregation of naphthalocyanine complex in concentrated solution (Figure 1). The shielding effect of π-extended peripheral 2-naphthyl groups results in upfield shift of αH proton signals in comparison with phenyl-substituted derivatives (Table 1). The positions of H_{Ar} protons are about the same for different aryl-substituted 2,3-naphthalocyanines in similar solvents. Introduction of bulky functional groups in aryl moieties, for instance SEt or CF_3 leads to deshielding of αH protons (Δδ is about 1 ppm, Table 1). The change of rigid C-C bond by C-O-C, for instance in phenoxy-substituted naphthalocyanines, have the greatest impact on position of αH proton signals.

By the analogy with initial dinitrile **2**, proton signals of H^{2} and H^{4} from naphthalocyanine moiety and H^{15} from 2-naphthyl groups appear as singlet, while other proton signals are multiplets.

Mass spectra of dinitrile **2** and naphthalocyanine complex **3** were measured using EI and MALDI TOF technique respectively. These spectra possess intense peaks of molecular ions (Figure S3 and S4). In the case of complex **3** the isotopic pattern distribution of molecular ion is coincided well with theoretically calculated one.

The high resolution MALDI TOF/TOF spectrum of naphthalocyanine complex demonstrated good agreement between the observed and calculated mass patterns (see Experimental section). The isotopic distribution of the molecular ion peak is almost equal to the theoretically calculated one (Figure S4).

The thermogravimetric study of the zinc complex **3** (Fig. S9) showed its reasonable stability up to 200°C. A slight mass change bellow 200°C can be attributed to the loss of coordinated water (m/z 18). Destruction of the complex skeleton (m/z 12; 16) at higher temperatures was accompanied with oxidation by oxygen (m/z 18 (H_2O); 30 (NO); 44 (CO_2); 46 (NO_2)). The most intense loss of weight was observed in the temperature range 200-600°C.

The UV-Vis spectrum of target naphthalocyanine complex **3** shows two main absorption bands: *B* band in UV region and *Q* band in the near IR region (Table 2). The *Q* band is the most intense and can be referred to the electron transition between HOMO and LUMO levels [3]; and its position is clearly solvent sensitive. For instance, compared to pyridine solution, a hypsochromic shift by 195 cm^{-1} (12 nm) of *Q* band was observed in THF solution. The *B* band position of **3** also showed bathochromic shift going from THF to pyridine (Δλ = 3 nm or Δν = 258 cm^{-1}). The shifts of *Q* and *B* bands of phthalocyanines and their analogues in nonpolar and polar solvents are typical and depend on refractive indices and dielectric constants of the solvents[22, 23].

In a common case, the *B* band positions lie near 340 nm for Zn complexes and 360 nm for Mg ones (Table 2).

Please do not adjust margins

Please do not adjust margins

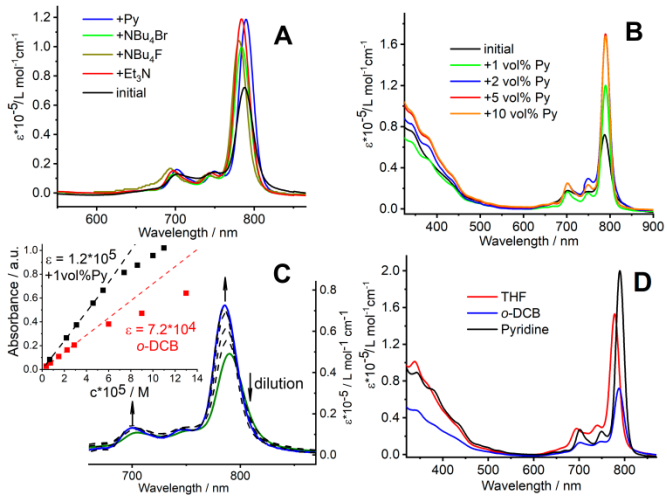

Figure 2. UV-Vis spectra of complex **3**: initial solution in *o*-DCB (black line, c= 3×10^{-5} M, *l* = 0.1 cm) and solutions after different additions (A). UV-Vis spectral changes during the addition of different vol% pyridine to solution of complex **3** in *o*-DCB (B). UV-Vis spectra of the solution of **3** in *o*-DCB at various concentrations (green line - c=1.3×10^{-4} M, blue line – c=1.5×10^{-5} M, dashed lines – intermediate concentrations). The inset depicts absorbance of *Q* band vs concentration. Dashed lines demonstrate Beer's law calibration curves (C). UV-Vis spectra of naphthalocyanine complex **3** in different solvents (D).

Table 2. UV-Vis data for compound **3**, some 2,3-naphthalocyanine complexes.

Compound	R	M	*B; Q* band positions, nm	Solvent	Reference
3	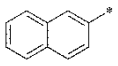	Zn	339; 778 342; 786 339; 790	THF *o*-DCB pyridine	Present paper
^{Ph8}NcZn	Ph	Zn	341; 772	THF	24
^{Ph8}NcMg	Ph	Mg	361; 772 349; 783	THF pyridine	9
^{PhO8}NcMg	PhO	Mg	359; 762	THF	12
$NcLi_2$	H	2Li	318; 736	acetone	25
NcZn	H	Zn	332; 767	DMSO	26
^{EtSPh8}NcZn		Zn	337; 775	THF	18
^{Ar8}NcMg	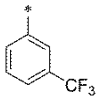	Mg	351; 770	THF	21
^{Ar8}NcZn		Zn	344; 771 350; 779	THF toluene	21

It was shown earlier, that the presence of $-CF_3$ moieties in phenyl substituents does not affect the *Q* band position. However, due to *+M* mesomeric effect of sulphur atom, the introduction of -SEt moieties results in a small bathochromic shift. Extension of the π-system of peripheral groups going from phenyl to 2-naphthyl results in a 100 cm^{-1} (6 nm) bathochromic shift of *Q* band position of **3** at 790 nm.

It was found that addition of even 1vol% pyridine or triethylamine (TEA) increases the Q/B band intensity ratio and makes *Q* band satellites more resolved (Figure 2). The FWHM for the *Q* band decreases from 29 to 20 nm in *o*-DCB and *o*-DCB + 1vol% pyridine respectively.

This phenomenon can be explained by two ways. First, the zinc's high affinity for nitrogen may lead to coordination of N-containing solvent to the central metal and disaggregation of naphthalocyanine molecules [27]. Second, TEA or pyridine may play a role of reducing agents for partially oxidized naphthalocyanine. In this last case, the initial *o*-DCB solution should consist of the mixture of neutral and oxidized forms of naphthalocyanine that may aggregate.

The addition of tetraalkylammonium halides (NBu_4Br and NBu_4F) or TEA affected the UV-Vis spectrum of the naphthalocyanine complex similarly to pyridine. This can be explained by coordination of nitrogen in TEA to the central metal (Zn) of the complex. In contrast, for tetraalkylammonium halides coordination of halide to central zinc ion can be realized. A similar phenomenon was earlier described for diazepinoporphyrazines[28, 29].

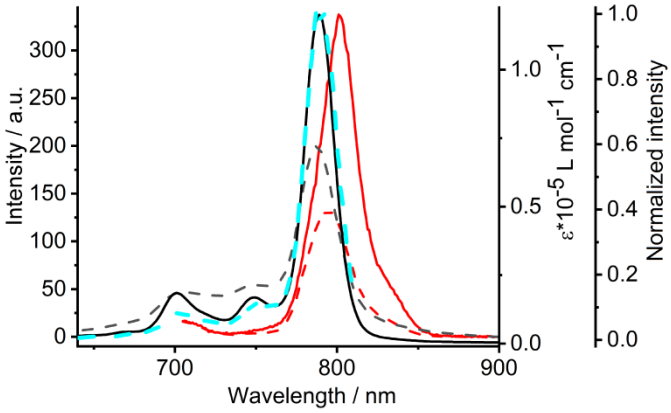

Figure 3. UV-Vis (black lines) and fluorescence (red lines, λ_{ex} = 695 nm, c=2.0×10^{-5} M) spectra of solution of compound **3** in *o*-DCB (dashed line) and solution in *o*-DCB after addition of 1 vol% pyridine (solid lines). Excitation spectra of solution of compound **3** in *o*-DCB λ_{em} = 820nm (light blue dashed line).

However, pyridine shows the most pronounced effect, which reaches maximum value under 2vol% pyridine addition.

In contrast, addition of 1 vol% reducing agents – $N_2H_4\times H_2O$, DMF or O-ligand (THF) did not change noticeably the UV-Vis spectrum of **3** in *o*-DCB.

The concentration study of absorption spectra was carried out. It was found, that for solution of **3** in *o*-DCB Beer's law is not obeyed above c_{lim} = 2×10^{-5} M (Figure 2C, Figure S7). The dilution of the initial solution from c = 1.3×10^{-4} M to c = 1.5×10^{-5} leads to an increase in the extinction coefficient by about 1.5 times.

This journal is © The Royal Society of Chemistry 20xx

Please do not adjust margins

Please do not adjust margins

Noteworthy, the dilution process was accompanied by a shift of the *Q* band maximum towards smaller wavelengths, a drop in intensity of a shoulder at 810 nm attributed to the absorbance of aggregates[30], and an increase in intensity of a *Q* band satellite at 700 nm.

In contrast, the addition of 1vol% pyridine leads to increase in c_{lim} till 6×10^{-5} M. Moreover, the spectral changes of *Q* band shape under the dilution are not so pronounced as for the initial *o*-DCB solution (Figure S7). Thus, it can be concluded that 2-naphthyl-substituted naphthalocyanine complex **3** possesses strong aggregation, which can be suppressed by N-containing agents or ternary ammonium salt due to steric hindrance or electrostatic repulsion.

Fluorescent properties were investigated for compound **3** in *o*-DCB. The emission maximum of complex **3** is observed at 801 nm and the Stokes shift of *Q* band equals 190 cm^{-1} (11 nm) (Figure 3). Such a small value of Stokes shift is typical for phthalocyanines [31, 32].

The fluorescence quantum yield (Φ_f) was measured for initial solution in *o*-DCB ($c = 2.0\times10^{-5}$ M) and in solution after addition of 1vol% pyridine. The enhancement of the fluorescence quantum yield was observed after the addition of pyridine. Further increase in quantum yield can be reached by dilution of initial *o*-DCB solution (Figure S8). The highest value of $\Phi_f\times100\% = 2.4\%$ was achieved when 1vol% pyridine was added to 1/16 diluted initial solution of compound **3**. This value is of the same order as that in unsubstituted zinc naphthalocyanine and about one order lower than in a phthalocyanine analogue [33]. A similar result of the experiment with dilution was observed for addition of NBu_4F (Figure S9).

The decrease in the fluorescence quantum yield at high concentrations can be explained by dynamic concentration quenching[34] and/or reabsorption effect[32] that can take place due to small Stokes shift of compound **3**.

From the definition of excitation spectra, the shape of an excitation and absorption spectrum of a monomeric naphthalocyanine complex should coincide [6]. However, for initial *o*-DCB solution, the resolution of *Q* band satellites is missed and broadening of the *Q* band is observed (Figure 3). The addition of 1 vol% pyridine to initial *o*-DCB solution results in complete resolution of two *Q* band satellites and absorption spectrum is the same as the excitation spectrum. Thus, comparison of the excitation and absorption spectra of different solutions allows concluding that pyridine additive plays a role of coordination rather than reducing agent.

The EPR spectra were measured for freshly prepared solution of compound **3** in *o*-DCB and after addition of 1 vol% pyridine (Figure S10). For both solutions only trace amounts of organic radicals were detected (a low intensity signal with g~2). Thus, the initial solution contained the neutral form of the naphthalocyanine and did not contain the mixture of the oxidized and neutral forms. However, the storage of the initial solution for one week resulted in appearance of a signal of an organic radical (g=1.998) in amount of around 30% of the initial concentration of compound **3**. It likely results from the typically high tendency of naphthalocyanine complexes to oxidation. Thus, solution of compound **3** is stable within a day and can be stored in the dark for a few days without self-oxidation.

The electrochemical properties of compound **3** were investigated using CV and SWV in *o*-DCB solution. Two oxidation and three reduction transitions were identified in CV with a small split of the first oxidation peak visible in SWV (Figure 4, black line). Table 3 lists the corresponding formal potentials ($E^{o'}$) and the difference between the first oxidation and first reduction potentials ($\Delta E = E^{o'}_{Ox}-E^{o'}_{Red1}$) that reflects the HOMO-LUMO gap of the complex.

In comparison with a phenyl-substituted phthalocyanine complex in *o*-DCB (^{Ph8}PcMg, Table 3), a strong shift by about 0.3 V towards lower values was observed for the first oxidation potential of the naphthalocyanines due to the well-known destabilization of the HOMO in naphthalocyanines compared to phthalocyanines[3]. Additionally, ΔE value of **3** is lower by 0.17 V (Table 3), which corresponds well to the expected decrease in the HOMO-LUMO gap in naphthalocyanines compared to phthalocyanines. In general, naphthalocyanine complex **3** shows facile oxidation and more difficult reduction in comparison with ^{Ph8}PcMg.

In comparison with a phenyl-substituted naphthalocyanine complex (^{Ph8}NcMg, Table 3), compound **3** shows essentially the same reduction potentials but a slightly higher first oxidation potential, which can be explained by a more pronounced electron-donating nature of the peripheral phenyl groups compared to naphthyl groups in **3**. Similarly, *tert*-butyl-substituted naphthalocyanine ($^{t\text{-}Bu4}$NcZn) has slightly more negative reduction and oxidation potentials compared to those for **3**. The ΔE values of **3** and naphthalocyanines reported in the literature are comparable (Table 3).

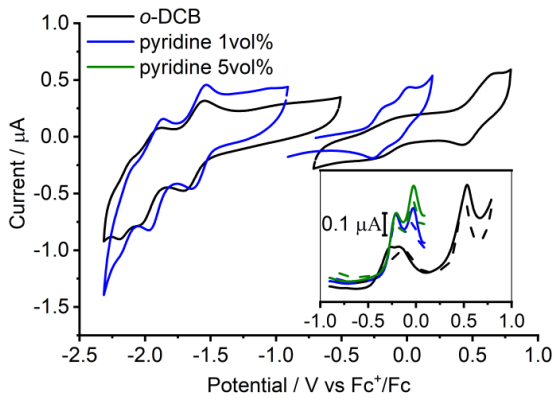

Figure 4. CVs of **3** in *o*-DCB containing 0.1 M $TBAPF_6$ as the supporting electrolyte. Scan rate = 0.1 V/s. **Insert**: SWVs of **3** (dash lines depict back scans).

Noteworthy, the first oxidation wave of **3** in CV was vague and suppressed, whereas other four redox waves were well-defined. Moreover, SWV showed a split in the region of the first oxidation (Figure 4, insert) which is rather unexpected, although a similar split was observed previously for *tert*-butyl substituted Cu naphthalocyanine[3] and *tert*-butyl substituted Zn phthalocyanine [35] complexes. Other authors speculated that two one-electron transitions might be involved [36] but they could not confirm it spectroelectrochemically.

Please do not adjust margins

Please do not adjust margins

Table 3. Formal reduction and oxidation potentials E°′ (vs Fc^+/Fc) in *o*-DCB containing 0.1 M $TBAPF_6$ in comparison to the literature data for phthalocyanine and naphthalocyanine analogues. Concentration of **3**, ca. 5×10^{-4} M. Potentials obtained by CV and SWV were identical within ±0.01V.

Compound/solvent	Red_3	Red_2	Red_1	Ox_1	Ox_2	Ox_3	ΔE
3/o-DCB	−2.15	−1.97	−1.63	−0.27, −0.18; −0.23[a]	+0.53	-	1.40[b]
3/*o*-DCB+1vol% py	−2.15	−1.92	−1.59	−0.22, −0.03	–	-	1.37[c]
^{Ph8}**NcMg**/ *o*-DCB [9]	−2.31	−1.99	−1.62	−0.29	+0.45	+0.93	1.33
$^{t\text{-}Bu4}$**NcZn**/ *o*-DCB [37]	-	–	-1.66	−0.29	–	-	1.37
$^{t\text{-}Bu4}$**NcCu**/ *o*-DCB [3]	-	-1.21[d]	-0.93[d]	+0.55[d]	+1.03[d]	-	1.48
$^{[CH2C(CH3)3]4}$**PcZn**/ *o*-DCB[38]	-	-2.04	-1.66	-0.02	+0.64	-	1.64
^{Ph8}**PcMg**/ *o*-DCB [9]	–	−1.90	−1.52	+0.05	+0.67	–	1.57

[a]The half-wave potential obtained by potential-resolved spectroelectrochemical titration (it matches the average of two potentials in the split).

[b]The potential obtained by spectroelectrochemical titration was used for calculation ΔE.

[c]The most negative potential of the split was used for calculation ΔE.

[d]potentials vs a silver-silver chloride reference electrode without correction to Fc^+/Fc

A split or a shoulder for the first oxidation transitions in Co(II) and Cu(II) phthalocyanines were also previously reported by Isago [39, 40] and Kobayashi [3]. The complication of the redox transition was attributed to two separate transitions, one in aggregates at a lower potential and another in a free monomer at a higher potential.

The concentration of the compound in our voltammeric measurements is high (0.5 mM) whereas the deviation from Beer's law starts from 0.06 mM (Figure 2C). Moreover, even for small concentrations, the absorbance of the complex is still suppressed in *o*-DCB compared to *o*-DCB containing disaggregating additives. Furthermore, as shown in Figure 2C, the *Q* band maximum shifts under dilution towards smaller wavelengths. This suggests that (1) phthalocyanine **3** is near fully aggregated in the conditions of the voltammetric measurements and (2) there should be noticeable interactions of macrocycles in the aggregates. The interactions may stabilize an oxidized molecule in the aggregates and make more difficult further oxidation. Thus, we attribute a split of the redox process to transitions in stable aggregates.

To further clarify the nature of the transitions in the region of the first oxidation, we conducted spectroelectrochemical titration that correlates changes in the optical spectrum with the potential applied. The UV-Vis spectroelectrochemical titration was performed in a diluted solution by controlled stepwise potential variation with 10 min equilibration for each step of 50 mV (Figure 5). The titration in the region of the first oxidation shows that the process is reversible, goes through a single set of isosbestic points (at 348, 445, 733 and 835 nm) and results in formation of a corresponding π-radical (the one-electron oxidized form) with the characteristic shape of the spectrum (with two bands at 695 and 845 nm) which is well documented for naphthalocyanines [17]. As the result of oxidation, the initial solution changed its color from olive to bright green due to strong absorbance at 650—750 nm. This contrasts with a previously described *tert*-butyl-substituted naphthalocyanine complex, which changes its color from green to red during the first oxidation process[17].

The shape of the titration curve along with a single set of isosbestic points and characteristic spectrum of the π-radical observed during the spectroelectrochemical experiment clearly indicates that the process in the region of the first oxidation is the single-electron transition with an average half-wave potential of −0.23 V. This potential matches the average value in the split and should result in the best estimation for ΔE.

Interestingly, addition of 1 or 5 vol% pyridine as a disaggregating agent in *o*-DCB solution of compound **3** resulted in two clear peaks separated by 0.19 V that is twice larger than the split in pure *o*-DCB. From the optical spectra we expect that pyridine may interfere with the structure of aggregates and release the monomer. The assignment of the transition was made in accordance with the expected HOMO-LUMO gap. Thus, the first oxidation was assigned to the monomer oxidation and the second to possible aggregates of the oxidized monomer with neutral molecule. This agrees with the same intensity of the peaks in the voltammograms. Potentials Red_1 and Red_2 are slightly shifted towards higher values in the presence of pyridine which agrees with the solvent effect reported for Al phthalocyanine[41]. The impact on the formal potentials suggests that pyridine indeed coordinates to the

Please do not adjust margins

Please do not adjust margins

metal center of **3** although aggregation cannot be excluded because Beer's law is not obeyed above 6×10^{-5} M (Figure 2C).

Unfortunately, spectroelectrochemical titration in the presence of pyridine was inconclusive since pyridine is electrochemically active at potentials of the first oxidation (background rises after addition of pyridine) and may interfere with long term measurements in the spectroelectrochemical cell. Nevertheless, we believe that the data regarding the effect of pyridine on the CV behavior of the naphthalocyanine might be interesting for the community since the effect is rather strong. Further systematic studies are needed to established detailed molecular mechanisms and behavior of a one-electron oxidized form of naphthalocyanines.

The use of spectroelectrochemical titration is popular for determination of the reduction potential of proteins but it has been largely ignored in the phthalocyanine community. The application of the spectroelectrochemical titration for estimation the half-wave potential of phthalocyanines with non-trivial CV behavior is undoubtedly a useful methodological tool.

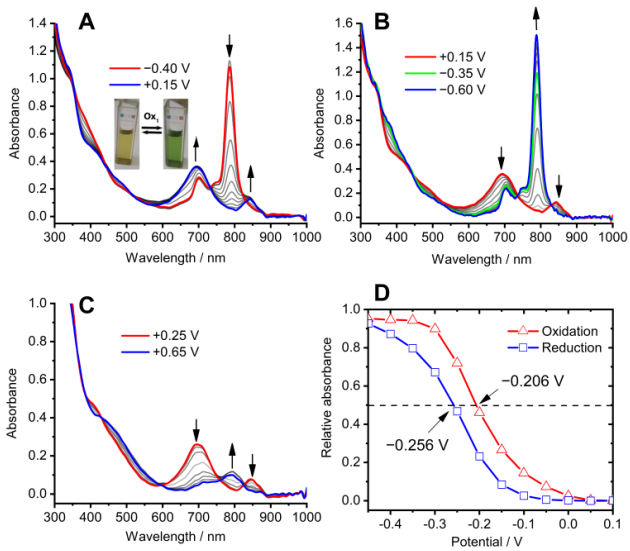

Figure 5. *In situ* UV-Vis spectral changes for solution of compound **3** (c ~ 7×10^{-5}) in *o*-DCB containing 0.1 M $TBAPF_6$ for oxidation in the region of Ox_1 (**A**); recovery of the initial neutral form of **3** from the first oxidation state (**B**); and oxidation in the region of the second oxidation Ox_2 (**C**). Absorption at 788 nm as a function of potential taken from the spectroelectrochemical titration in the region of the first oxidation process (**D**). All potentials are given vs Fc^+/Fc.

Experimental

Materials and methods

All reagents and solvents were obtained or distilled according to standard procedures. 2-Naphthylboronic acid (Sigma-Aldrich, ≥95.0%) was used as received. 6,7-Dibromonaphthalene-2,3-dicarbonitrile was synthesized according to the published procedure [42]. $Zn(OAc)_2\times2H_2O$ was dried immediately before use for 4 h at 70°C.

Thin-layer chromatography (TLC) was performed using Merck Aluminium Oxide F_{254} neutral flexible plates. UV-Vis absorption spectra were recorded on a ThermoSpectronic Helios-α spectrophotometer using quartz cells. Matrix assisted laser desorption/ionization time-of-flight (MALDI-TOF) mass-spectra were taken on a Bruker Autoflex II mass spectrometer with α-cyano-4-hydroxycinnamic acid (CHCA) as the matrix. High-resolution MALDI mass spectra were registered on a Bruker ULTRAFLEX II TOF/TOF instrument.

^{1}H and ^{13}C and ^{1}H-^{13}C NMR spectra were recorded on Bruker Avance 400 (400.13 MHz for ^{1}H and 100.61 MHz for ^{13}C) and Bruker Avance 600 (600.13 MHz for ^{1}H and 150.92 MHz for ^{13}C) spectrometers. Chemical shifts are given in ppm relative to $SiMe_4$.

IR spectra were measured using an IR 200 Thermonicolet spectrometer with a spectral resolution $\Delta\lambda = 4$ cm^{-1}.

Fluorescence, excitation and UV/Vis spectra were recorded on a Varian Cary Eclipse spectrofluorometer and Hitachi U-2900 spectrophotometer using quartz cells (10 x 10 mm). The comparative method using a solution of fluorescein in 0.01 M KOH in 95 % ethanol as the standard was applied to determine the fluorescence quantum yields (Φ_f(fluorescein) = 0.97 with λ_{ex} = 470 nm) [43]. The calculation of fluorescence quantum yield (Φ_f) was made according to the following equation [44]:

$$\Phi_f^S = \frac{G^S A_\lambda^R n_{DCB}^2}{G^R A_\lambda^S n_{etanol}^2} \times \Phi_f^R$$

where G is the integrated emission area, n is the refractive index of the solvent, A_λ is the absorbance at the excited wavelength, and Φ_f is the fluorescence quantum yields.

EPR spectra were recorded at Bruker EMX 500 spectrometer of X-range. Spectra were recorded at room temperature. The microwave power used did not cause saturation of the EPR signals. The modulation amplitude was chosen in such a way that no distortion of spectral lines was observed. The value of frequency modulation was 100 kHz.

Electrochemical measurements were carried out in o-dichlorobenzene (*o*-DCB, 99%, J&K) containing 0.1 M $TBAPF_6$ (Sigma-Aldrich) using Autolab 302 potentiostat controlled by Nova 1.11 (Metrohm Autolab B.V., The Netherlands). Cyclic voltammetry (CV) and square wave voltammetry (SWV) were performed in a conventional three-electrode cell with Pt-disk (2.0 mm in diameter) working and Pt-rod counter electrodes. A double junction Ag|AgCl (1 M LiCl in EtOH) reference electrode (Metrohm, 6.0726.110) was connected to the solution through a salt bridge containing *o*-DCB, 0.1 M $TBAPF_6$. Ferrocenium$^+$/ferrocene (Fc^+/Fc) was used as internal reference for correction liquid junction potentials ($E^{o\prime}$ = +0.51 vs Ag|AgCl used). The solution was purged with argon for at least 20 min before measurements.

Spectroelectrochemical studies were conducted in *o*-DCB containing 0.1 M $TBAPF_6$ using Avantes AvaSpec 2048 spectrometer coupled with Autolab 101 potentiostat/galvanostat (Metrohm-Autolab), a thin-layer quartz spectroelectrochemical cell (optical path of 1.0 mm), a

Please do not adjust margins

Please do not adjust margins

Pt mesh working, a Pt wire counter and an Ag|Ag^+ reference electrodes. The difference between the Ag|Ag^+ and Ag|AgCl reference electrodes in *o*-DCB was measured before the experiment to recalculate all potentials vs Fc^+/Fc. Spectra were recorded automatically over 10 min time interval for each potential step of 50 mV.

Preparation of 6,7-*bis*(2-naphthyl)naphthalene-2,3-dicarbonitrile 2:

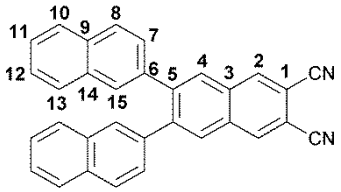

A mixture of 6,7-dibromonaphthalene-2,3-dicarbonitrile **1** (0.5 g, 1.49 mmol), 2-naphthylboronic acid (1.54 g, 8.95 mmol) and a saturated aqueous solution of K_2CO_3 (1.23 g, 8.95 mmol) were stirred in 29 mL of boiling mixture 1,4-dioxane:acetonitrile (2.6:1, V:V) under argon. The dichloro-*bis*(triphenylphosphine) palladium compound (0.02 g, 0.029 mmol) was added after boiling the solvent (b.p.=84°C, 760 mm Hg). The reaction was carried out for 4 h (TLC-control: Al_2O_3, ethyl acetate:*n*-hexane, 1:10, V:V). The reaction mixture was cooled to room temperature and 150 mL of water was added. The product was collected by extraction with ethyl acetate and dried with $CaCl_2$. The residue was purified by gradient chromatography using benzene and then ethyl acetate as the eluent. The resulting compound (fraction moved by ethyl acetate) was dissolved by benzene and then *n*-hexane was added. The resulting precipitate was dried at room temperature, yielding target compound **2** (0.41 g, 64%). The compound is decomposed under melting (m.p.=225 °C). R_f =0.43 (ethyl acetate:*n*-hexane, 1:10, V:V). ^{1}H NMR δ_H (400.13 MHz, [D_6]DMSO) 7.16-7.19 (2H, dd, $J(H^7,H^8)$=8.5 Hz, $J(H^7,H^{15})$=1.7 Hz, H^7); 7.51 (2H, d, $J(H^{11},H^{12})$=3.3 Hz, H^{11}); 7.52 (2H, d, $J(H^{11},H^{12})$=3.3 Hz, H^{12}); 7.69 (2H, d, $J(H^7,H^8)$=8.5 Hz, H^8); 7.83-7.85 (2H, dd, J(H^{10}, H^{11})=6.1 Hz, J(H^{10}, H^{12})=3.5 Hz, H^{10}); 7.86-7.88 (2H, dd, J(H^{13}, H^{12})=6.1 Hz, J(H^{13}, H^{11})=3.5 Hz, H^{13}); 8.02 (2H, s, H^{15}); 8.41 (2H, s, H^4); 8.96 (2H, c, H^2). ^{13}C NMR δ_{13} (150.90 MHz, [D_6]DMSO) 108.97 (C^1); 116.47 (CN); 126.47 (C^{11}); 126.51 (C^{12}); 127.34 (C^7); 127.38 (C^8); 127.46 (C^{10}); 127.97 (C^{13}); 128.40 (C^{15}); 130.61 (C^4); 131.89 (C^9); 132.20 (C^3); 132.74 (C^{14}); 136.37 (C^2); 137.18 (C^6); 143.13 (C^5). IR ν (KBr): 2231 cm^{-1} (st CN). MS-EI (I/Imax, %) m/z: 430 [M, 100%]; calculated for $C_{32}H_{18}N_2$ 430.1470, found for [M] 430.1470.

Preparation of 3,4,12,13,21,22,30,31-octa-(2-naphthyl)-2,3-naphthalocyaninato zinc 3:

A mixture of 6,7-*bis*(2-naphthyl)naphthalene-2,3-dicarbonitrile (100.0 mg, 0.23 mmol), $Zn(OAc)_2\times2H_2O$ (25.0 mg, 0.12 mmol) and 1,8-diazabicycloundec-7-ene (0.2 mL) were stirred in 2.5 mL of boiling isoamyl alcohol under argon. The reaction was carried out for 6 h. The reaction mixture was cooled to room temperature and a MeOH:H_2O (20:1 V/V) mixture was added. The precipitate was filtered and washed with a MeOH:H_2O (20:1 V/V) mixture and then MeOH, yielding **3** (90.0 mg, 87%). UV-Vis λ_{max} (*o*-DCB+1%Py)/nm 342 (lgε 4.74), 701 (4.24), 750 (4.20) and 790 (5.10). ^{1}H NMR δ_H (600.13 MHz, THF-d_8, 47°C) 7.23-7.24 (8H, m, H^2); 7.39-7.42 (16H, m, H^5, H^6); 7.58-7.60 (8H, m, H^3); 7.74-7.77 (16H, m, H^4, H^7); 7.98 (8H, s, H^1); 8.35 (8H, s, βH); 8.45 (8H, s, αH). IR (ZnSe): ν (cm^{-1}): 1374-1624 (γ pyrrole), 3053 (st CH_{Ar}). MS (MALDI-TOF) m/z: 1658 ([M-Naphthyl]$^+$, 16%), 1784 ([M]$^+$, 100%); calculated for $C_{128}H_{72}N_8Zn$ 1784.5171, found for [M] 1784.5020.

Conclusions

Novel zinc 2,3-naphthalocyanine with bulky 2-naphthyl groups was obtained in a high yield starting from 6,7-dibromonaphthalene-2,3-dicarbonitrile in two steps through Suzuki cross-coupling and template synthesis (total yield = 56%). The bathochromic shift of *Q* band of compound 3 was the highest in the row ^{PhO8}NcMg < ^{Ph8}NcMg < ^{EtSPh8}NcZn < compound **3**.

The spectral and electrochemical studies indicated that compound **3** is prone to aggregation in *o*-DCB, which is significantly suppressed in the presence of pyridine (> 2%) or tetraalkylammonium halides probably due to their coordination to the metal center.

The electrochemical and spectroelectrochemical studies demonstrated an electron-withdrawing nature of 2-naphthyl groups at peripheral positions, which destabilizes the HOMO relative to the LUMO and hence results in the unusual color change upon oxidation.

Conflicts of interest

There are no conflicts to declare.

Acknowledgements

Synthesis, identification and optical studies of target compounds were supported by the Russian Science Foundation Grant № 19-73-00099. Electrochemical and spectroelectrochemical measurements were supported by ERA.Net RUS Plus Plasmon Electrolight and FWO funding (RFBR №18-53-76006 ERA). Fluorescence studies were supported by the Council under the President of the Russian Federation for State Support of Young Scientists and Leading Scientific Schools (Grant MD-3847.2019.3). The NMR spectroscopic measurements were carried out in the Laboratory of Magnetic Tomography and Spectroscopy, Faculty of Fundamental Medicine of Moscow State University.

References

1. E. A. Lukyanets and V. N. Nemykin, *Journal of Porphyrins and Phthalocyanines*, 2010, **14**, 1-40.
2. V. N. Nemykin and E. A. Lukyanets, *ARKIVOC*, 2010, 136-208.

This journal is © The Royal Society of Chemistry 20xx

Please do not adjust margins

Please do not adjust margins

3. N. Kobayashi, S.-i. Nakajima, H. Ogata and T. Fukuda, *Chemistry – A European Journal*, 2004, **10**, 6294-6312.
4. P. A. Firey and M. A. J. Rodgers, *Photochemistry and Photobiology*, 1987, **45**, 535-538.
5. M. Shopova, D. Woehrle, V. Mantareva and S. Mueller, *Journal of Biomedical Optics*, 1999, **4**.
6. L. Luan, L. Ding, W. Zhang, J. Shi, X. Yu and W. Liu, *Bioorganic & Medicinal Chemistry Letters*, 2013, **23**, 3775-3779.
7. M. Kimura, H. Nomoto, H. Suzuki, T. Ikeuchi, H. Matsuzaki, T. N. Murakami, A. Furube, N. Masaki, M. J. Griffith and S. Mori, *Chemistry – A European Journal*, 2013, **19**, 7496-7502.
8. Y. Shen, F. Zheng, W. Cheng, F. Gu, J. Zhang and Y. Xia, *Semiconductor Science and Technology*, 2010, **25**, 065016.
9. T. V. Dubinina, S. A. Trashin, N. E. Borisova, I. A. Boginskaya, L. G. Tomilova and N. S. Zefirov, *Dyes and Pigments*, 2012, **93**, 1471-1480.
10. W. Zheng, B.-B. Wang, J.-C. Lai, C.-Z. Wan, X.-R. Lu, C.-H. Li and X.-Z. You, *Journal of Materials Chemistry C*, 2015, **3**, 3072-3080.
11. T. V. Magdesieva, I. V. Zhukov, L. G. Tomilova, O. V. Korenchenko, I. P. Kalashnikova and K. P. Butin, *Russian Chemical Bulletin*, 2001, **50**, 396-403.
12. T. V. Dubinina, R. A. Piskovoi, A. Y. Tolbin, V. E. Pushkarev, M. Y. Vagin, L. G. Tomilova and N. S. Zefirov, *Russian Chemical Bulletin*, 2008, **57**, 1912-1919.
13. G. Schnurpfeil, A. K. Sobbi, W. Spiller, H. Kliesch and D. WÖhrle, *Journal of Porphyrins and Phthalocyanines*, 1997, **01**, 159-167.
14. R. Bonnett and G. Martínez, *Tetrahedron*, 2001, **57**, 9513-9547.
15. A. G. Martynov, E. A. Safonova, A. Y. Tsivadze and Y. G. Gorbunova, *Coordination Chemistry Reviews*, 2019, **387**, 325-347.
16. E. A. Safonova, A. G. Martynov, S. E. Nefedov, G. A. Kirakosyan, Y. G. Gorbunova and A. Y. Tsivadze, *Inorganic Chemistry*, 2016, **55**, 2450-2459.
17. V. N. Nemykin, N. A. Kostromina, N. B. Subbotin and S. V. Volkov, *Russian Chemical Bulletin*, 1996, **45**, 89-92.
18. T. V. Dubinina, P. I. Tychinsky, N. E. Borisova, S. S. Maklakov, M. V. Sedova, A. D. Kosov, L. G. Tomilova and N. S. Zefirov, *Dyes and Pigments*, 2017, **144**, 41-47.
19. T. V. Dubinina, M. S. Belousov, S. S. Maklakov, V. I. Chernichkin, M. V. Sedova, V. A. Tafeenko, N. E. Borisova and L. G. Tomilova, *Dyes and Pigments*, 2019, **170**, 107655.
20. T. V. Dubinina, K. V. Paramonova, S. A. Trashin, N. E. Borisova, L. G. Tomilova and N. S. Zefirov, *Dalton Transactions*, 2014, **43**, 2799-2809.
21. S. Vagin and M. Hanack, *European Journal of Organic Chemistry*, 2003, **2003**, 2661-2669.
22. M. Yousaf and M. Lazzouni, *Dyes and Pigments*, 1995, **28**, 69-75.
23. F. Ghani, J. Kristen and H. Riegler, *Journal of Chemical & Engineering Data*, 2012, **57**, 439-449.
24. A. V. Kazak, M. Marchenkova, T. Dubinina, A. I. Smirnova, L. G. Tomilova, A. Rogachev, D. Chausov, A. A. Stsiapanau and N. Usol'tseva, *New Journal of Chemistry*, 2020, DOI: 10.1039/C9NJ06041C.
25. F. Guyon, A. Pondaven, P. Guenot and M. L'Her, *Inorganic Chemistry*, 1994, **33**, 4787-4793.
26. A. Vogler and H. Kunkely, *Inorganica Chimica Acta*, 1980, **44**, L209-L210.
27. F.-J. Yang, X. Fang, H.-Y. Yu and J.-D. Wang, *Acta Crystallographica Section C*, 2008, **64**, m375-m377.
28. P. A. Stuzhin, P. Tarakanov, S. Shiryaeva, A. Zimenkova, O. I. Koifman, E. Viola, M. P. Donzello and C. Ercolani, *Journal of Porphyrins and Phthalocyanines*, 2012, **16**, 968-976.
29. P. A. Tarakanov, E. N. Tarakanova, P. V. Dorovatovskii, Y. V. Zubavichus, V. N. Khrustalev, S. A. Trashin, K. De Wael, M. E. Neganova, D. V. Mischenko, J. L. Sessler, P. A. Stuzhin, V. E. Pushkarev and L. G. Tomilova, *Dalton Transactions*, 2018, **47**, 14169-14173.
30. E. A. Safonova, M. A. Polovkova, A. G. Martynov, Y. G. Gorbunova and A. Y. Tsivadze, *Dalton Transactions*, 2018, **47**, 15226-15231.
31. E. A. Kuzmina, T. V. Dubinina, A. V. Zasedatelev, A. V. Baranikov, M. I. Makedonskaya, T. B. Egorova and L. G. Tomilova, *Polyhedron*, 2017, **135**, 41-48.
32. S. Dhami, A. J. D. Mello, G. Rumbles, S. M. Bishop, D. Phillips and A. Beeby, *Photochemistry and Photobiology*, 1995, **61**, 341-346.
33. P. Tau, A. O. Ogunsipe, S. Maree, M. D. Maree and T. Nyokong, *Journal of Porphyrins and Phthalocyanines*, 2003, **07**, 439-446.
34. Z. Petrášek and D. Phillips, *Photochemical & Photobiological Sciences*, 2003, **2**, 236-244.
35. T. Nyokong, Z. Gasyna and M. J. Stillman, *Inorganic Chemistry*, 1987, **26**, 548-553.
36. M. E. El-Khouly, L. M. Rogers, M. E. Zandler, G. Suresh, M. Fujitsuka, O. Ito and F. D'Souza, *ChemPhysChem*, 2003, **4**, 474-481.
37. R. Chitta, A. S. D. Sandanayaka, A. L. Schumacher, L. D'Souza, Y. Araki, O. Ito and F. D'Souza, *The Journal of Physical Chemistry C*, 2007, **111**, 6947-6955.
38. V. Manivannan, W. A. Nevin, C. C. Leznoff and A. B. P. Lever, *Journal of Coordination Chemistry*, 1988, **19**, 139-158.
39. H. Isago, C. C. Leznoff, M. F. Ryan, R. A. Metcalfe, R. Davids and A. B. P. Lever, *Bulletin of the Chemical Society of Japan*, 1998, **71**, 1039-1047.
40. N. Kobayashi, H. Miwa, H. Isago and T. Tomura, *Inorganic Chemistry*, 1999, **38**, 479-485.
41. Z. Ou, J. Shen and K. M. Kadish, *Inorganic Chemistry*, 2006, **45**, 9569-9579.
42. T. V. Dubinina, A. V. Ivanov, N. E. Borisova, S. A. Trashin, S. I. Gurskiy, L. G. Tomilova and N. S. Zefirov, *Inorganica Chimica Acta*, 2010, **363**, 1869-1878.
43. P. G. Seybold, M. Gouterman and J. Callis, *Photochemistry and Photobiology*, 1969, **9**, 229-242.
44. S. Fery-Forgues and D. Lavabre, *Journal of Chemical Education*, 1999, **76**, 1260.

Please do not adjust margins